

DOI: 10.1002/anie.200503915

Imaging Proteins in Membranes of Living Cells by High-Resolution Scanning Ion Conductance Microscopy***Andrew I. Shevchuk, Gregory I. Frolenkov, Daniel Sánchez, Peter S. James, Noah Freedman, Max J. Lab, Roy Jones, David Klenerman,* and Yuri E. Korchev**

Advances in imaging and microscopy have driven many discoveries in biology over the past century. Electron-microscopy-based techniques (for example, freeze-fracture, freeze-etching, and/or immunogold labeling^[1]) have provided a wealth of evidence that cell plasma membranes are organized into structural and functional microdomains.^[2] However, these techniques are only applicable to fixed or frozen cells, thereby precluding live imaging of functionally important membrane structures in living cells. Lower-resolution optical methods such as fluorescent-molecule video imaging^[3] and single-particle tracking of gold-conjugated ligands^[4] have been used successfully to follow the dynamics of specific molecules in the plasma membrane of living cells. The disadvantage of these tracking methods is that they require labeling and hence do not image the relative position of the

[*] Dr. D. Klenerman

Department of Chemistry, Cambridge University
Cambridge, CB21EW (UK)
Fax: (+44) 1223-336-362
E-mail: dk10012@cam.ac.uk

Dr. A. I. Shevchuk, Dr. D. Sánchez, Prof. Dr. M. J. Lab,
Prof. Dr. Y. E. Korchev
Division of Medicine, Imperial College London
MRC Clinical Sciences Centre
London W120NN (UK)
Fax: (+44) 208-383-8306
E-mail: y.korchev@ic.ac.uk

Dr. G. I. Frolenkov
Department of Physiology, University of Kentucky
MS-508, Chandler Medical Center
800 Rose Street, Lexington, KY 40536-0298 (USA)

P. S. James, Dr. R. Jones
Laboratory of Molecular Signalling
The Babraham Institute
Cambridge, CB24AT (UK)

N. Freedman
Ionscope Limited
The London BioScience Innovation Centre
2 Royal College Street, London NW1 0NH (UK)

[**] This work was funded by the Biotechnology and Biological Sciences Research Council (UK). The development of the high-resolution scanning ion conductance microscopy instrument was performed in collaboration with Ionscope Limited (UK).



Supporting information for this article is available on the WWW under <http://www.angewandte.org> or from the author.

tagged reporter with respect to the surrounding proteins and other membrane structures.

In contrast to the techniques above, scanning probe microscopy (SPM) does not require extensive specimen preparation and potentially could be used for high-resolution imaging in living cells. The most developed version of these techniques, atomic force microscopy (AFM), can image proteins on hard substrates and has also been successfully applied for imaging living cells,^[5,6] but so far it has not been possible to achieve molecular resolution on the surface of living cells. This is due to difficulties in controlling the probe–sample separation over the soft and responsive cell surface. However, a special form of SPM, scanning ion conductance microscopy (SICM), originally developed by Hansma and co-workers,^[7] has been successfully adapted by us for living-cell imaging.^[8]

SICM is based on a scanned nanopipette and uses the ion current that flows between an electrode in the pipette and a bath electrode for feedback control of the pipette–sample distance. This distance is maintained at the pipette inner radius during the scan, thereby allowing noncontact imaging of the cell surface in physiological buffer with a resolution determined by the pipette inner radius.^[9,10] Essentially there is a hemisphere, with the same radius as the pipette inner radius, centered at the pipette tip that senses the surface by reduction in the flow of ion current. Unlike the situation in AFM, this means that the sensing is both vertically under the pipette and also laterally, thereby helping to prevent the pipette walls from touching the cell surface.

Herein, we describe scanning that utilizes very narrow quartz pipettes with an inner diameter of the tip of about 13 nm. The extremely small diameter of the pipettes, custom-designed software, and enhanced mechanical stability of the system have allowed us to improve the resolution of SICM^[8] by an order of magnitude. We demonstrate this by imaging individual proteins crystallized on a flat surface or protruding at the external surface of the plasma membrane of a living cell (spermatozoon), whilst maintaining the noncontact advantage of SICM. These advances have made it possible to directly image protein complexes in the membrane of a living cell.

Figure 1 A shows a schematic diagram of the experimental setup. The scanning nanopipette is mounted on a computer-controlled piezo device that provides motion in the vertical direction. The position of the pipette relative to the sample strongly influences the ion current flowing through the pipette; this is then measured by a current amplifier. The

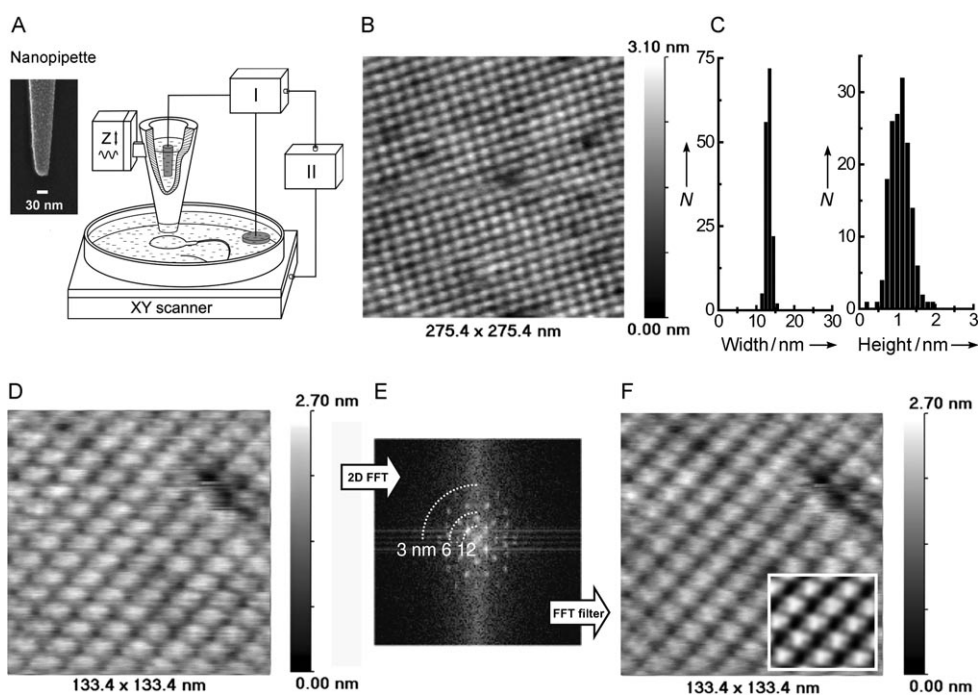


Figure 1. Verification of the SICM resolution by direct imaging of single proteins. A) Schematic diagram of the high-resolution SICM experimental setup (I: ion-current amplifier; II: scanner control). For details see text. The inset shows an SEM image of the tip of a typical nanopipette used for SICM imaging. B) A typical raw SICM image of the S-layer protein of *Bacillus sphaericus* on a mica surface. C) S-layer protein width and height distributions based on SICM measurements. D) Smaller-range SICM scan of the S-layer protein. E) 2D FFT of the image in (D). F) FFT-filtered image produced from (D) by selecting nine pairs of spots in the power spectrum in (E). The inset shows the correlation-averaged image of S-layer proteins calculated from the FFT-filtered data.

pipette's vertical position is then readjusted by the computer to maintain constant nanopipette tip–sample separation, at approximately one pipette radius from the surface, by using the amplified ion current as the feedback signal. The topographical image is generated by measuring the movements of the pipette in the z direction, as the sample is raster-scanned under the pipette in the x and y directions. A quantitative analysis shows that the opening of an ion channel underneath the pipette has a negligible effect on the topography measured (see the Supporting Information). The apparent outer diameter of the tip of the typical quartz nanopipette used for SICM imaging was about 30 nm (including a 2.5-nm platinum coating), as observed by scanning electron microscopy (SEM; Figure 1 A, inset). Assuming that the inner/outer diameter ratio of the capillary template is preserved during the pulling process, we estimate the inner diameter of the quartz pipette tip to be about 12.5 nm.

The SICM resolution was determined by imaging a monolayer of S-layer (cell surface layer) proteins from *Bacillus sphaericus* CCM 2177 on a mica surface (Figure 1 B). The monolayer consists of identical 120-kDa protein subunits, 13.1 nm apart, arranged in a square lattice. Individual protein molecules are clearly identifiable in the unprocessed SICM image and we could also detect the occasional protein missing from the array. Repeated scans of the sample gave identical images, a result indicating that the nanopipette is not

disrupting the protein layer. A statistical analysis of the width and height of the proteins showed a narrow distribution of widths centered at (13.19 ± 0.04) nm (Figure 1C). This is in good agreement with previous measurements of 13.1 nm for the S-layer protein lattice spacing.^[11,12] The pipette is too wide to enter the holes in the lattice and hence it can only record the tops of the protein subunits, thereby measuring a height change of (1.058 ± 0.013) nm.^[11]

A higher-resolution unprocessed SICM image is shown in Figure 1D and a computed two-dimensional fast Fourier transform (FFT) of this image is shown in Figure 1E. The dashed-line quarter circles mark spatial frequencies corresponding to 12, 6, and 3 nm resolution, respectively. The spatial frequency at which it is still possible to see distinct features can be used to estimate the SICM resolution. Since there are discrete spots between the 3 and 6 nm rings this indicates that the lateral resolution is 3–6 nm. After FFT filtering (Figure 1F) and correlation averaging (Figure 1F, inset), it is possible to also identify some structural features of individual S-layer proteins. Similar triangular structures have been observed in processed AFM images by Wetzer et al.^[13]

Having established that the technique has sufficient resolution to image individual protein molecules, we then applied it to the plasma membrane of a living specialized cell, a boar spermatozoon. Spermatozoa were chosen as an example of a highly polarized cell whose plasma membrane is compartmentalized into functionally and topographically different domains, known as the anterior acrosome, equatorial segment, equatorial subsegment, postacrosome, midpiece, and principal piece.^[14] In order to first characterize the

specimen by a proven technique, an SEM image of the equatorial segment of a boar spermatozoon, after a spontaneous acrosome reaction in physiological buffer, was taken, along with a high-resolution image of the subsegment (see the Supporting Information).

Figure 2A shows an SICM image of the head and anterior midpiece of a living boar spermatozoon that has initiated a spontaneous acrosome reaction in physiological buffer. The boxed area in Figure 2A, shown at higher resolution in Figure 2B, corresponds to the equatorial segment and its contained subsegment. SICM images at this resolution are similar to SEM and AFM images and reveal protrusions of similar size. The topographical features shown were not observed in non-acrosome-reacted spermatozoa (Figure 2C), a result that is in good agreement with the fact that the equatorial segment only becomes fusogenic after the acrosome reaction when new antigenic epitopes appear as a result of membrane reorganization.^[15,16] At higher resolution, however, on the acrosome-reacted sperm, these protrusions appear as small projecting particles (Figure 2D). There are stable regions that are clearly identifiable in the two scans taken 10 min apart (Figure 2D, examples highlighted with dashed lines).

Analysis of the distribution of the width (Figure 2E) and height (Figure 2F) of the particles revealed two populations. The diameter of the small particles was ≈ 14 nm and of the large particles was ≈ 30 nm (Figure 2E). The heterogeneous nature of the particles is reflected in the frequency distribution of their heights (Figure 2F). The densities of the small and large complexes were 380 and 220 per μm^2 , respectively.

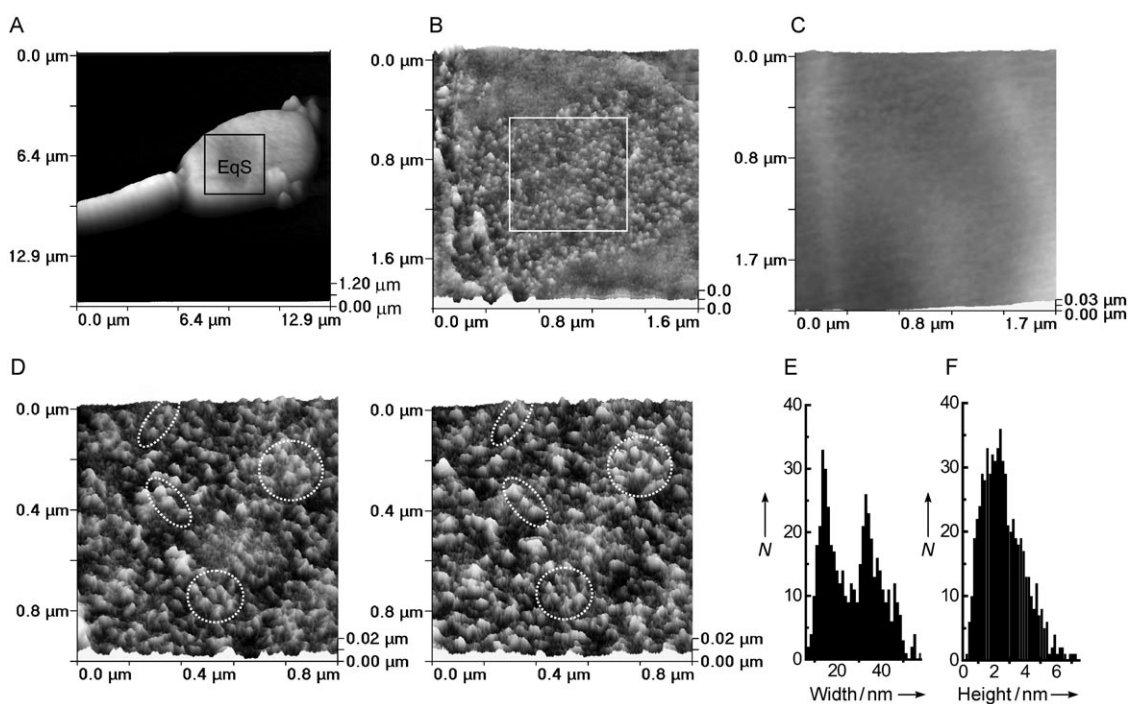


Figure 2. Changes in the organization of protein complexes on the surface of living spermatozoa imaged by SICM. A) Low-resolution SICM image of a boar spermatozoon undergoing a spontaneous acrosome reaction. B) A higher-resolution image of the equatorial segment (EqS) region of the sperm marked in (A) reveals flat and more convoluted areas (subsegments) of the membrane. C) A low-resolution SICM image of a boar spermatozoon prior to the spontaneous acrosome reaction reveals a featureless surface. D) Two consecutive images of the area boxed in (B) recorded 10 min apart. The distribution of E) the widths and F) the heights of individual proteins calculated from various SICM topographical images.

The particles that we have imaged here are reminiscent of the intramembranous particles (IMPs) described in freeze-fracture studies of boar sperm plasma membranes.^[17,18] Two types of IMPs, ≈ 8 nm and > 10 nm in diameter, were present on both the protoplasmic (P) and external (E) faces of the bilayer and were most numerous over the anterior acrosomal and equatorial segment domains. The densities of the smaller and larger IMPs were 670 and 270 per μm^2 , respectively, values that are close to the coverage of the proteins estimated by our SICM measurements. IMPs are generally thought to represent transmembrane proteins or protein complexes.^[19] Many have been identified as ion channels (for example, the band 3 anion transporter in erythrocytes^[20]) or multisubunit receptors (for example, acetylcholine receptors^[21]) and found to interact with the cytoskeleton. In this respect, it may be significant that voltage-dependent Ca^{2+} ion channels and actin have been localized to the equatorial segment of boar and human sperm.^[22,23] On the basis of their size, density, and distribution, it is likely that most of the features shown in Figure 2D are the topographical images of the external portions of proteins or protein complexes. The differences in size of the IMPs detected by freeze-fracture studies^[17] and the proteins seen in the SICM images may reflect the effects of fixation or instrumentation, or both, while the differences in density could be due to the fact that some IMPs do not extend a sufficient distance beyond the outer leaflet of the bilayer to be detectable in the SICM image.

Figure 3A presents topographical images, taken 10 min apart, of an area of membrane where the vast majority of proteins are stable and only two small areas exhibit aggregation (marked with dashed lines). To facilitate visualization of these changes, artificial color was applied to both images, the early one in red and the later image in green. In the overlay image (Figure 3B), yellow color appears in those places where the position and shape of the proteins did not change. Figure 3C and D show areas with fewer stable proteins and provide examples of what appear to be structural (large circle) and orientational (small circle) changes. In Figure 3E and F, lateral shift of a relatively large horseshoe-shaped protein complex (top left, uncircled) is apparent, along with evidence for disassembly (top-right circle) and appearance de novo of other components or fast diffusion (central circle). Note that the majority of proteins remained largely unchanged (yellow color in the overlay images), a result indicating that the illustrated dynamics are not a measurement artifact. Also, in control experiments in which spermatozoa were fixed in 4% formaldehyde, no structural changes or rearrangements were observed over a similar timeframe (data not shown).

Thus, by imaging a living spermatozoon at different time intervals, we have found that some proteins are remarkably stable in position, possibly because they are anchored to the cytoskeleton which permits only reorientation and structural changes. Other proteins disappear from or appear on the

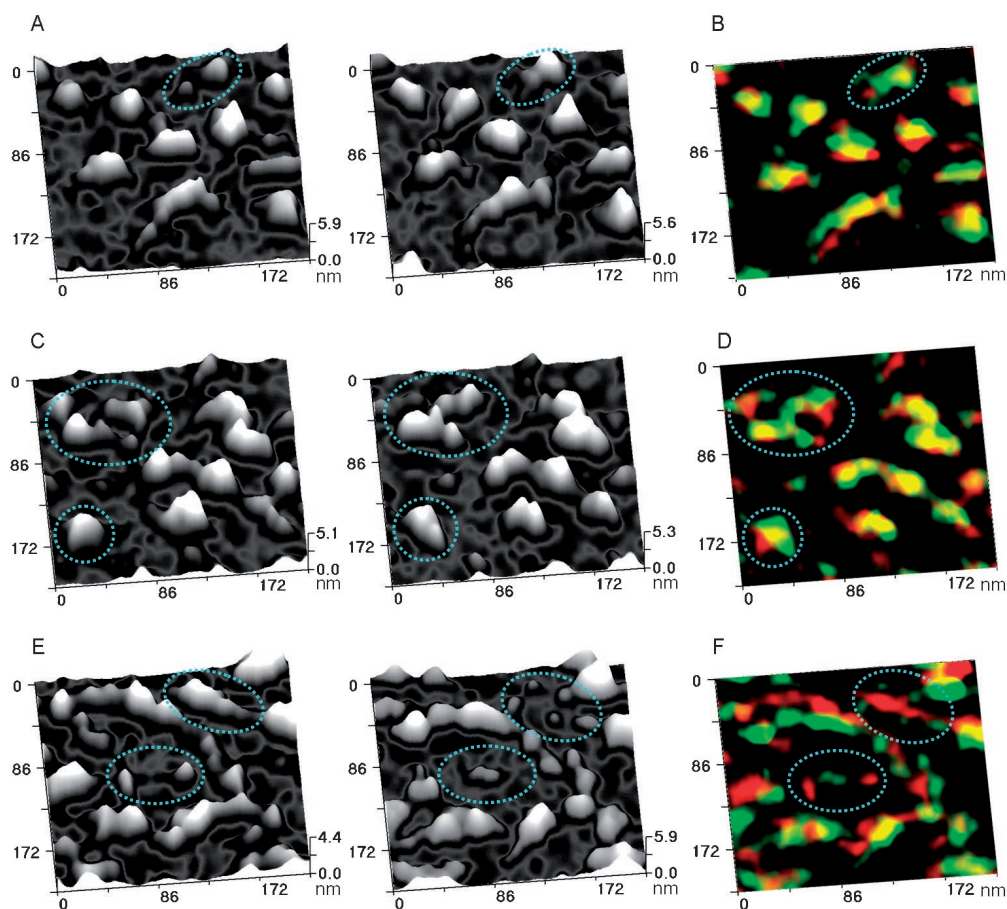


Figure 3. Direct imaging by SICM of the dynamics of single proteins and protein complexes in the membrane overlying the equatorial subsegment (representative zoomed images from Figure 2D). For details of what is shown in A–F, see text.

external surface of the membrane, thereby suggesting removal, insertion, or very fast diffusion^[24] that is beyond the current temporal resolution of SICM. Immobile membrane proteins have been postulated as diffusion barriers on cell surfaces.^[4] Our measurements provide evidence for these immobile proteins. These experiments demonstrate that SICM can follow changes in the structure of the surface of living cells at the resolution of individual protein complexes. There is a trade-off between scan speed and image quality in these experiments; hence, imaging of smaller regions and improvements such as modulation at higher frequency should allow faster events to be imaged.

In summary, we have shown that SICM can be performed at a sufficient resolution on living cells to image fixed or slowly diffusing individual protein complexes in the plasma membrane and to follow their reorganization over time. In general such proteins are likely to be present on highly structured cells where specific functions are associated with particular specialized regions or domains. The capability to image living cells at a resolution sufficient for the identification of protein complexes, directly and without labeling, opens up a wealth of new possibilities in membrane biology, such as the spatial mapping of slowly diffusing proteins (for example, ion channels) and the direct imaging of the organization of microdomains or diffusion barriers.

Received: November 4, 2005

Published online: February 28, 2006

Keywords: cells · imaging · membrane proteins · membranes · scanning probe microscopy

- [1] P. Rock, M. Allietta, W. W. Young, Jr., T. E. Thompson, T. W. Tillack, *Biochemistry* **1990**, *29*, 8484–8490.
- [2] K. Simons, E. Ikonen, *Nature* **1997**, *387*, 569–572.
- [3] G. J. Schutz, M. Sonnleitner, P. Hinterdorfer, H. Schindler, *Mol. Membr. Biol.* **2000**, *17*, 17–29.
- [4] K. Murase, T. Fujiwara, Y. Umemura, K. Suzuki, R. Iino, H. Yamashita, M. Saito, H. Murakoshi, K. Ritchie, A. Kusumi, *Biophys. J.* **2004**, *86*, 4075–4093.
- [5] A. Sharma, K. I. Anderson, D. J. Muller, *FEBS Lett.* **2005**, *579*, 2001–2008.
- [6] M. K. Tsilimbaris, E. Lesniewska, S. Lydataki, C. Le Grimellec, J. P. Goudonnet, I. G. Pallikaris, *Invest. Ophthalmol. Visual Sci.* **2000**, *41*, 680–686.
- [7] P. K. Hansma, B. Drake, O. Marti, S. A. Gould, C. B. Prater, *Science* **1989**, *243*, 641–643.
- [8] Y. E. Korchev, C. L. Bashford, M. Milovanovic, I. Vodyanoy, M. J. Lab, *Biophys. J.* **1997**, *73*, 653–658.
- [9] Y. E. Korchev, M. Milovanovic, C. L. Bashford, D. C. Bennett, E. V. Sviderskaya, I. Vodyanoy, M. J. Lab, *J. Microsc.* **1997**, *188*, 17–23.
- [10] J. Gorelik, A. I. Shevchuk, G. I. Frolenkov, I. A. Diakonov, M. J. Lab, C. J. Kros, G. P. Richardson, I. Vodyanoy, C. R. Edwards, D. Klenerman, Y. E. Korchev, *Proc. Natl. Acad. Sci. USA* **2003**, *100*, 5819–5822.
- [11] E. S. Gyoryvary, O. Stein, D. Pum, U. B. Sleytr, *J. Microsc.* **2003**, *212*, 300–306.
- [12] N. Ilk, C. Vollenkle, E. M. Egelseer, A. Breitwieser, U. B. Sleytr, M. Sara, *Appl. Environ. Microbiol.* **2002**, *68*, 3251–3260.
- [13] B. Wetzler, D. Pum, U. B. Sleytr, *J. Struct. Biol.* **1997**, *119*, 123–128.
- [14] D. J. Ellis, S. Shadan, P. S. James, R. M. Henderson, J. M. Michael Edwardson, A. Hutchings, R. Jones, *J. Struct. Biol.* **2002**, *138*, 187–198.
- [15] H. Takano, R. Yanagimachi, U. A. Urch, *Zygote* **1993**, *1*, 79–91.
- [16] C. A. Allen, D. P. Green, *J. Cell Sci.* **1995**, *108*, 767–777.
- [17] F. Suzuki-Toyota, Y. Itoh, K. Naito, *Dev. Growth Differ.* **2000**, *42*, 265–273.
- [18] F. W. Kan, D. S. Pinto, *J. Histochem. Cytochem.* **1987**, *35*, 1069–1078.
- [19] D. S. Friend, L. Orci, A. Perrelet, R. Yanagimachi, *J. Cell Biol.* **1977**, *74*, 561–577.
- [20] T. Inoue, A. Kanzaki, A. Yawata, A. Tsuji, K. Ata, N. Okamoto, H. Wada, I. Higo, T. Sugihara, O. Yamada, *Int. J. Hematol.* **1994**, *59*, 157–175.
- [21] A. G. Yee, G. D. Fischbach, M. J. Karnovsky, *Proc. Natl. Acad. Sci. USA* **1978**, *75*, 3004–3008.
- [22] S. Benoff, *Hum. Fertil.* **1999**, *2*, 42–55.
- [23] M. Camatini, A. Casale, *Gamete Res.* **1987**, *17*, 97–105.
- [24] A. E. Cowan, D. E. Koppel, L. A. Vargas, G. R. Hunnicutt, *Dev. Biol.* **2001**, *236*, 502–509.